Broadband Metamaterial Reflectors for Polarization Manipulation based on Cross/Ring Resonators

Zhao ZHANG, Xiangyu CAO, Jun GAO, Sijia LI

Information and Navigation College, Air Force Engineering University, Xi'an 710077, China

bjzhangzhao323@126.com, xiangyucaokdy@163.com

Manuscript received January 19, 2016

Abstract. *We presented the investigation of broadband metamaterial reflector for polarization manipulation based on cross/ring resonators. It is demonstrated that the metamaterial reflector can convert the linearly polarized incident wave to its cross polarized wave or circularly polarized wave. Due to the multiple resonances at neighboring frequencies, the proposed reflector presents broadband property and high efficiency. The measured fraction bandwidth of cross polarization conversion is 55.5% with efficiency higher than 80%. Furthermore, a broadband circular polarizer is designed by adjusting the dimension parameters and the measured fraction bandwidth exceeds 30%.*

Keywords

Metamaterial reflector, polarization manipulation, multiple resonances, broadband

1. Introduction

Polarization plays an important role among all the properties of electromagnetic wave, and great efforts have been made to realize the polarization manipulation. In recent years, metamaterials have provided various choices for polarization manipulation [1–5]. Based on anisotropy or optical activity, the linearly polarized incident wave can be converted to its cross polarized or circularly polarized wave by metamaterials [6–9]. For instance, cross polarization converters have been designed by the anisotropic high impedance surfaces which could cause different phase delays for different polarization waves [8], [9]. Furthermore, by controlling the amplitude and phase delay of reflected or transmitted orthogonally polarized wave, the circular polarizers are proposed [10–15]. Chiral metamaterials have also been utilized to manipulate the polarization and obtain asymmetric transmission [16–19].

Broadband metamaterial reflector is always a hot research area in polarization manipulation. Due to the intrinsic resonance modes of metamaterial structure, broadband metamaterial reflector can be designed using multiple resonances or resonance hybridizations. Feng et al. proposed a cross polarization rotator based on multi-order resonances [20]. The polarization conversion bandwidth reaches 54.5%, while the cross polarization conversion efficiency is just above 56%. Shi et al. proposed a cross polarization converter using resonance hybridizations [21]. Conversion efficiency is higher than 80%, while the bandwidth is only 38%. Till now, the bandwidth expansion with high efficiency for polarization manipulation, especially the linear to circular polarization conversion, is still one of the main research interests.

In this work, we propose a metamaterial reflector to realize the broadband polarization manipulation, including cross polarization conversion and linear to circular polarization conversion. The proposed reflector consists of the cross and square ring resonators. The resonances of cross couples with the resonances of square ring, which generates multiple resonances and broadband polarization manipulation. The designed cross polarization convertor operates in 11.2~19.8 GHz with a fraction bandwidth of 55.5% and an efficiency higher than 80%. Furthermore, adjusting the dimensions of the resonator will change the amplitude and phase of reflected orthogonally polarized wave. Then, a broadband circular polarizer is designed and the fraction bandwidth of axis ratio (AR) less than 3 dB exceeds 30%.

2. Design and Analysis

Figure 1(a) shows the geometry of a unit cell for the proposed metamaterial reflector. The proposed reflector consists of the top layer of a cross/square-ring resonator and the bottom layer of a perfect electric conductor separated by a dielectric layer. On the top layer, the cross is placed at the center of the square ring, and its two arms with different lengths point toward the diagonal direction. The bottom conductive layer ensures that most of the incident power is reflected. The metamaterial reflector is designed, simulated and optimized using High Frequency Structure Simulator (HFSS) based on finite-element analysis. The periodic boundary conditions and Floquet port are utilized to simulate the infinite periodic cells as shown in Fig. 1(b).

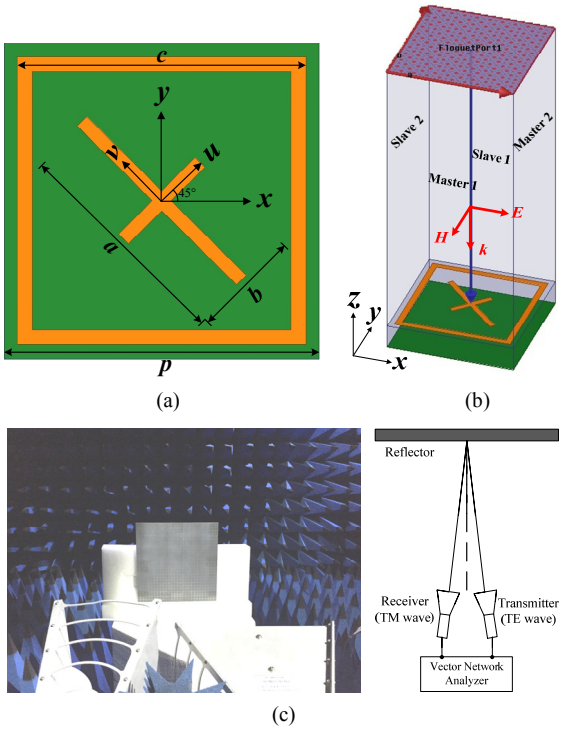

Fig. 1. Geometry of the reflector: (a) Top view; (b) Simulation model; (c) Fabricated sample and measurement setup.

To understand the principle of multiple resonances, we model the structure as an anisotropic structure with two symmetrical axis, *u*-axis and *v*-axis, as shown in Fig. 1(a). Under normal incidence, it is possible for the cross arms to excite individual resonances by choosing the polarization angle of the incident linearly polarized wave to be 0° or 90° with respect to *u*-axis. For intermediate angles, both resonances are excited, so multiple resonances can be excited by properly choosing the incidence polarization angle and arm length of the cross. On the other hand, the ring is a highly tunable structure and supports multipolar modes excited by oblique incidence, retardation effects or coupling with other structure. By placing the cross inside the square ring, the symmetry of ring is broke, and the resonances of the ring will couple with modes of the cross, which excites the multiple resonances.

The polarization manipulation is realized by controlling the amplitude and phase of the two orthogonal components of the reflected wave. The normal incident *x* polarized or *y* polarized electric fields can be decomposed into two orthogonal components along the *u*-axis and *v*-axis with the same amplitude, respectively. Then, different resonant modes are excited, and a phase difference between the reflected orthogonal components along the *u*-axis and *v*-axis is generated. If the phase difference is 180°, the reflected wave is linearly polarized and the incident *x* or *y* polarized wave is converted to its cross polarized wave. In another case, if the phase difference is designed to be ±90° and reflected orthogonal components have the same amplitude, the incident linearly polarized wave is converted to a circularly polarized wave.

3. Simulation and Discussion

3.1 Broadband Cross Polarization Convertor

As a cross polarization convertor, the thickness and relative dielectric constant are designed as 4 mm and 2.2, respectively. The fabricated sample consists of 28 × 28 unit cells with a total area of 294 mm × 294 mm as shown in Fig. 1(c). Due to the symmetry along *u*-axis, we take the incident *x* polarized wave for the analysis and discussion. Because the bottom layer is perfect electric conductor, the transmission of the proposed reflector is zero. Define $R_{xx} = |E_{rx}/E_{ix}|$ and $R_{yx} = |E_{ry}/E_{ix}|$ to represent the reflection ratio of *x*-to-*x* and *x*-to-*y* polarization conversions under the *x* polarized normal incidence.

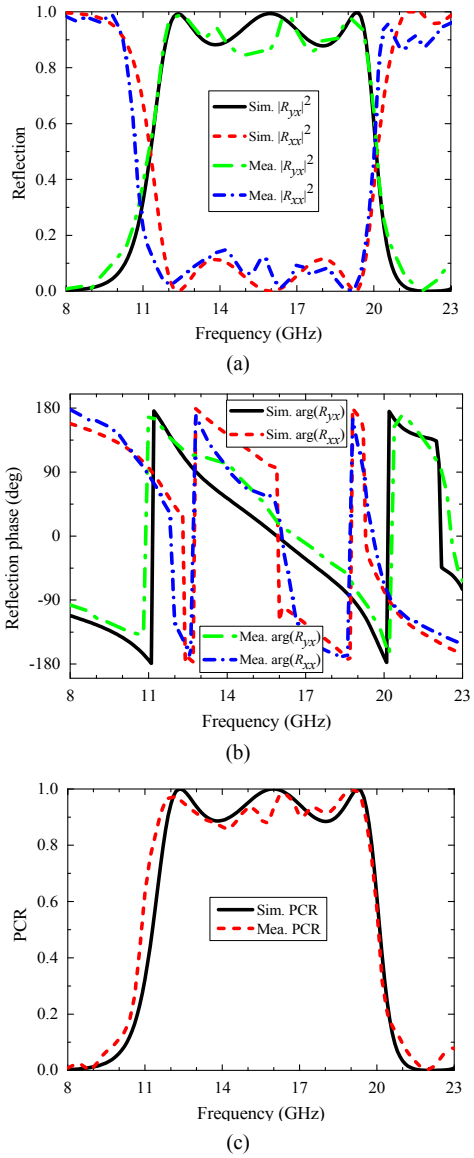

Fig. 2. Simulated and measured results of the broadband cross polarization convertor: (a) $|R_{yx}|^2$ and $|R_{xx}|^2$; (b) φ; (c) PCR. The corresponding geometrical parameters are designed as: p = 10.5 mm, a = 7.5 mm, b = 3.6 mm, and c = 9.6 mm.

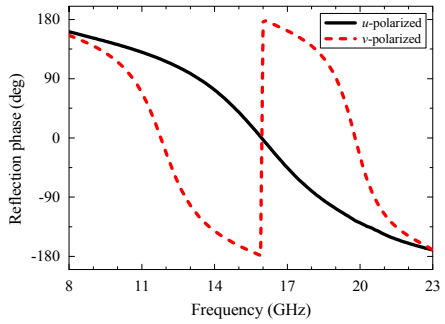

Fig. 3. The reflection phase for the incident wave polarized along *u*-axis and *v*-axis.

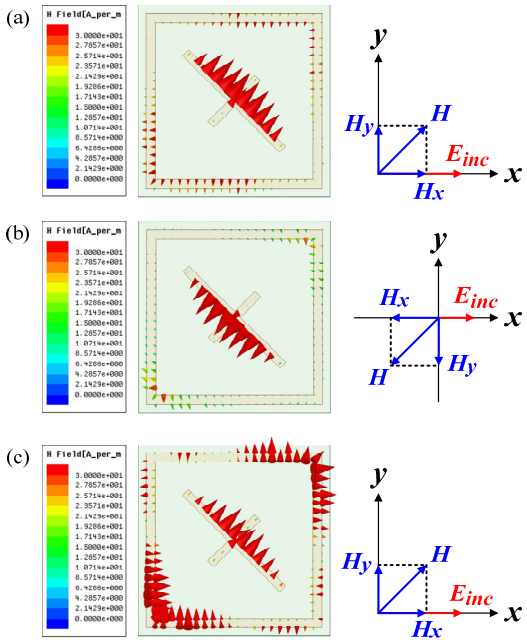

Fig. 4. The induced surface magnetic field distributions: (a) 12.4 GHz; (b) 16.0 GHz; (c) 19.3 GHz.

Cross polarization convertor	Fraction bandwidth	PCR	Period
In [20]	54.5%	56%	0.19λ
In [21]	38%	80%	0.5λ
In [22]	70%	68.6%	0.43λ
Our work	55.5%	80%	0.54λ

Tab. 1. Performance comparison.

Figure 2(a) shows the simulated and measured normalized amplitude of the reflected power. According to the law of energy conservation, the equation $|R_{yx}|^2 + |R_{xx}|^2 = 1$ is true for this lossless case. We can find that there exist three peak values of $|R_{yx}|^2$ that are close to 1.0. Namely, at the three resonant frequencies, 12.4, 16.0 and 19.3 GHz, almost all the power of the incident wave is converted to its cross-polarized wave. From 11.7 to 19.8 GHz, the power of the reflected cross-polarized wave is larger than 0.8, while the one of the reflected co-polarized wave is lower than 0.1. So, the incident wave is converted to its cross polarized wave with a fraction bandwidth of 51.4% and an efficiency higher than 80%. Figure 2(b) shows the reflection phase of R_{yx} and R_{xx}. At 11.3 GHz and 20.1 GHz, phase difference $\Delta\varphi$ between R_{yx} and R_{xx} is ±90° and $|R_{yx}|^2$ is equal to $|R_{xx}|^2$, which indicates a circularly polarized reflected wave. In other frequency band, $\Delta\varphi$ has little significance because $|R_{xx}|^2$ is insignificant compared to $|R_{yx}|^2$, which means the wave is linearly polarized. Polarization conversion ratio (PCR) is introduced to demonstrate the polarization conversion efficiency. It is defined as $PCR = R_{yx}^2/(R_{xx}^2 + R_{yx}^2)$. The simulated PCR is shown in Fig. 2(c). It can be seen PCR is higher than 80% from 11.7 to 19.8 GHz and achieves 1.0 at the three resonant frequencies which means nearly all energy of the incident *x* polarized wave is converted to *y* polarized one at the three resonant frequencies.

To understand the mechanism of broadband polarization conversion, the reflection phase for the incident wave polarization along *u*-axis and *v*-axis is shown in Fig. 3. We can see the incident *u*-polarized and *v*-polarized waves have different reflection phase. From 12 to 19 GHz, the phase difference is about 180°. In other words, under the *x* or *y* polarized normal incidences, the reflected orthogonal components along *u*-axis and *v*-axis have the same amplitude but a 180° phase difference. Thus, the total reflected wave has a 90° rotation angle to the total incident wave, and the incident wave is converted to its cross polarized wave. Meanwhile, at 11.3 and 20.1 GHz, the phase differences of the reflected waves are ±90°, respectively. Thus, the linearly polarized incident wave is converted to a circularly polarized reflected wave at 11.3 and 20.1 GHz. However, the conversion from linear to circular polarization just at two frequency points has little significance. The later section will demonstrate a broadband circular polarizer based on the above structure.

To better understand the physical mechanism of the polarization conversion, the induced surface magnetic field distributions under the *x* polarized incidence are depicted in Fig. 4. At the resonance frequency of 12.4 GHz, the induced magnetic field $\boldsymbol{H}$ is along the up-right direction, as shown in Fig. 4(a). Decompose $\boldsymbol{H}$ into two orthogonal components $\boldsymbol{H}_\mathbf{x}$ and $\boldsymbol{H}_\mathbf{y}$ along *x*-axis and *y*-axis, respectively. The component $\boldsymbol{H}_\mathbf{y}$ is perpendicular to the incident electric field $\boldsymbol{E}_\mathbf{inc}$. Then $\boldsymbol{H}_\mathbf{y}$ does not contribute to the polarization conversion because there is no cross-coupling between $\boldsymbol{H}_\mathbf{y}$ and $\boldsymbol{E}_\mathbf{inc}$. On the other hand, the component $\boldsymbol{H}_\mathbf{x}$ is parallel to the incident electric field $\boldsymbol{E}_\mathbf{inc}$. It will induce an electric field that is perpendicular to $\boldsymbol{E}_\mathbf{inc}$, which results in the polarization conversion. The same physical mechanism occurred at the resonant frequency of 16.0 and 19.3 GHz, which are shown in Fig. 4(b) and 4(c). The magnetic field component parallel to the incident electric field contributes to the polarization conversion.

Table 1 lists the performance comparison between several cross polarization convertors. Compared with the other three convertors, the proposed convertor has a wide operation band and high efficiency at the same time. Meanwhile, the period is 0.54λ at the center frequency and 0.69λ at 19.8 GHz, which are smaller than the wavelength. Thus, there is no grating lobe problem.

3.2 Broadband Circular Polarizer

In this section, a broadband circular polarizer is designed to demonstrate the application of the proposed reflector in the liner-to-circular polarization conversion. The dimensions of the structure in Fig. 1(a) is optimized aiming at controlling the two orthogonal components of the reflected wave to have the same amplitude and a 90° phase difference in a broadband frequency range. The thickness and relative dielectric constant are 3.5 mm and 2.65, respectively. Other parameters are also optimized.

To evaluate the performance of the proposed circular polarizer, the polarization azimuth angle τ with respect to x-axis and ellipticity χ are calculated as [23]

$$\tau = \frac{1}{2}\arctan\left(\frac{2R\cos(\Delta\varphi)}{1-R^2}\right), \tag{1}$$

$$\chi = \frac{1}{2}\arcsin\left(\frac{2R\sin(\Delta\varphi)}{1+R^2}\right) \tag{2}$$

where $R = |R_{yx}|/|R_{xx}|$ and $\Delta\varphi = \arg(R_{yx}) - \arg(R_{xx})$. Then, the axis ratio is calculated as

$$AR = \left|\frac{1}{\tan\chi}\right|. \tag{3}$$

For the circularly polarized wave, χ should be ±45° and AR should be 1. If $\chi = 45°$, it means the reflected wave is a left handed circularly polarized wave. If $\chi = -45°$, then the reflected wave is a right handed circularly polarized wave.

The simulated results under the x polarized incidence are shown in Fig. 5. From Fig. 5(a) and 5(b) we can see the reflected orthogonal components almost have the same amplitude and their phase difference is about 90°. This result accords with the features of circularly polarized wave. Furthermore, as shown in Fig. 5(d), the ellipticity χ is about –45° from 12 to 15 GHz, which indicates a right handed circularly polarized wave. Namely, the proposed structure converts the linearly polarized incident wave to the circularly polarized wave in a broad band. Figure 5(e) shows that the bandwidth of $AR < 3$ dB covers from 11.5 to 15.6 GHz with a fraction bandwidth of 30.3%. What's more, at 9.6 and 18.6 GHz, the ellipticity χ is 45°, which means a left handed circularly polarized wave.

To illustrate the polarization state of reflected wave, the polarization ellipses at different frequencies are shown in Fig. 6. The polarization azimuth angle is obtained from Fig. 5(c). At 11.5 and 15.7 GHz, the upper and lower side frequency of working band, the reflected waves are right handed elliptical and the major axes of ellipse are close to y-axis and x-axis, respectively. At 12.6, 13.8 and 15 GHz, AR reaches minimal values close to 0 dB. So the reflected waves are right handed circular and the major axis of ellipse is tilted on 22.3°, 40.2° and 69.6° with respect to x-axis, respectively. It should be pointed out that, the left handed or right handed polarization state of the reflected circularly polarized wave is depend on the polarization state of the incident wave. If the incident wave is changed to be y polarized wave, the reflected wave will be left handed circularly polarized wave.

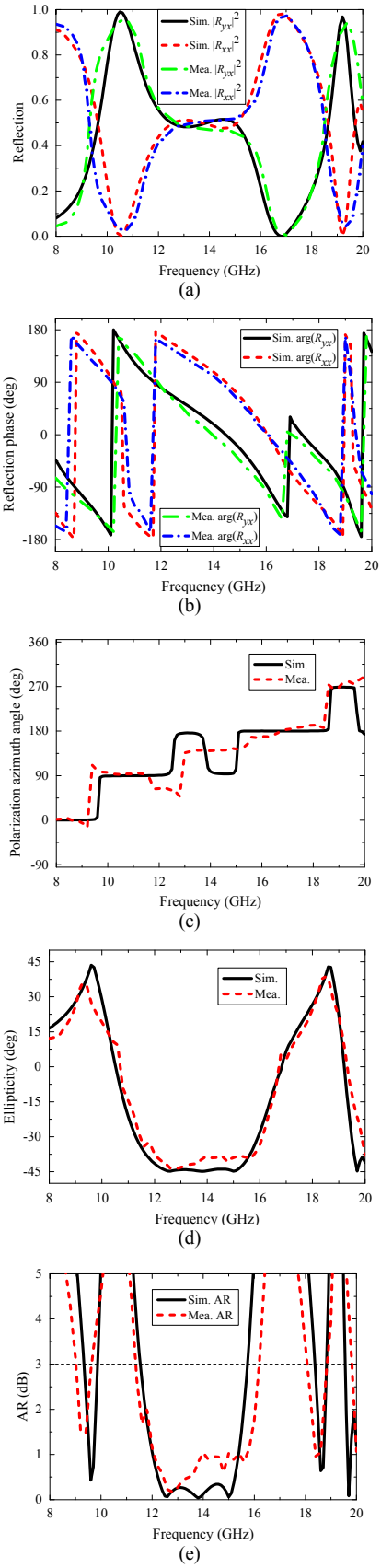

Fig. 5. Simulated and measured results of the broadband circular polarizer: (a) $|R_{yx}|^2$ and $|R_{xx}|^2$; (b) φ; (c) τ; (d) χ; (e) AR. The corresponding geometrical parameters are designed as: $p = 13.2$ mm, $a = 7.8$ mm, $b = 4$ mm, and $c = 7.4$ mm.

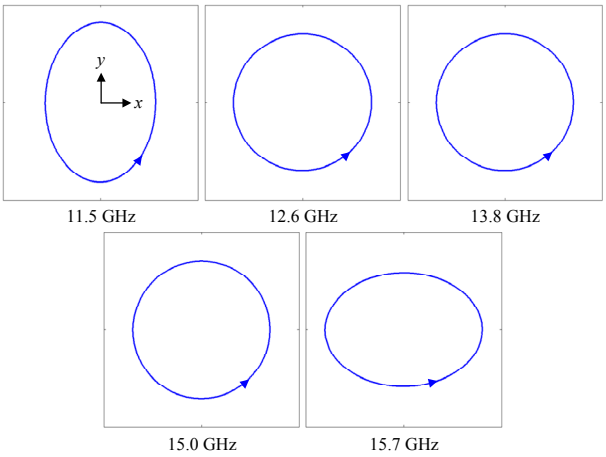

Fig. 6. Polarization ellipses (waves are coming out of the paper).

4. Fabrication and Measurement

To verify the simulation results, the proposed cross polarization convertor has been fabricated and measured in a microwave anechoic chamber as shown in Fig. 1(c). A vector network analyzer and two broadband linearly polarized horn antennas were used to constitute the test system. The time-domain gating strategy was used to eliminate the undesirable signals. The sample was placed at a distance of 50 cm away from the horn antennas. The horn antenna is capable of receiving both vertical and horizontal polarizations by rotating the receiving horn antenna 0° and 90°, respectively. In this way, if one of the antennas is perpendicular to the other one with the center at the same height, the cross-polarization reflection can be measured. A metal sheet with the same size as the sample was also measured for the sake of normalization. The measured results are compared with the simulation results as shown in Fig. 2 and Fig. 5. The reasonable agreement between simulation and measurement validates the application of the proposed reflector in broadband polarization conversion.

5. Conclusion

A metamaterial reflector, composed of cross and square ring structure has been investigated for broadband polarization manipulation by simulation and experiment. The combination of cross and square ring breaks the azimuthal symmetry and leads to multiple resonances. Polarization manipulation is realized by controlling the amplitude and phase of the two orthogonal components of the reflected wave. Measured results show that the proposed reflector not only can be used to realize the cross polarization conversion with fraction bandwidth of 55.5% and efficiency higher than 80%, but also can be used to convert liner polarization to circular polarization with a 30.3% AR bandwidth. Measured results are in good agreement with the simulated ones. Theoretically and experimentally, the proposed reflector has the function of broadband polarization manipulation.

Acknowledgments

This work is supported by the National Natural Science Foundation of China (No. 61271100, No. 61471389 and No. 61501494) and the Doctoral Foundation of Air Force Engineering University (No. KGD080914002). Authors also thank reviewers for their valuable comments.

References

[1] ZHAO, J., XIAO, B., HUANG, X., et al. Multiple-band reflective polarization converter based on complementary L-shaped metamaterial. *Microwave and Optical Technology Letters*, 2015, vol. 57, no. 4, p. 978–983. ISSN: 1098-2760. DOI: 10.1002/mop.29003

[2] BARBUTO, M., BILOTTI, F., TOSCANO, A. Novel waveguide components based on complementary electrically small resonators. *Photonics and Nanostructures - Fundamentals and Applications*, 2014, vol. 12, no. 4, p. 284–290. ISSN: 1569-4410. DOI: 10.1016/j.photonics.2014.03.005

[3] BARBUTO, M., TROTTA, F., BILOTTI, F., et al. A combined bandpass filter and polarization transformer for horn antennas. *IEEE Antennas and Wireless Propagation Letters*, 2013, vol. 12, p. 1065–1068. ISSN: 1536-1225. DOI: 10.1109/LAWP.2013.2280151

[4] SHI, H., ZHANG, A., ZHENG, S., et al. Dual-band polarization angle independent 90° polarization rotator using twisted electric-field-coupled resonators. *Applied Physics Letters*, 2014, vol. 104, no. 3. p. 034102. ISSN: 0003-6951. DOI: 10.1063/1.4863227

[5] CONG, L., CAO, W., ZHANG, X., et al. A perfect metamaterial polarization rotator. *Applied Physics Letters*, 2013, vol. 103, no. 17, p. 171107. ISSN: 0003-6951. DOI: 10.1063/1.4826536

[6] JIA, Y., ZHANG, Y., DONG, X., et al. Complementary chiral metasurface with strong broadband optical activity and enhanced transmission. *Applied Physics Letters*, 2014, vol. 104, no. 1, p. 011108. ISSN: 0003-6951. DOI: 10.1063/1.4861422

[7] PU, M., CHEN, P., WANG, Y., et al. Anisotropic meta-mirror for achromatic electromagnetic polarization manipulation. *Applied Physics Letters*, 2013, vol. 102, no. 13, p. 131906. ISSN: 0003-6951. DOI: 10.1063/1.4799162

[8] DOUMANIS, E., GOUSSETIS, G., GÓMEZ-TORNERO, J. L., et al. Anisotropic impedance surfaces for linear to circular polarization conversion. *IEEE Transactions on Antennas and Propagation*, 2012, vol. 60, no. 1, p. 212–219. ISSN: 0018926X. DOI: 10.1109/TAP.2011.2167920

[9] YAN, S., VANDENBOSCH, G. A. E. Compact circular polarizer based on chiral twisted double split-ring resonator. *Applied Physics Letters*, 2013, vol. 102, no. 10, p. 103503. ISSN: 0003-6951. DOI: 10.1063/1.4794940

[10] MARTINEZ-LOPEZ, L., RODRIGUEZ-CUEVAS, J., MARTINEZ-LOPEZ, J. I., et al. A multilayer circular polarizer based on bisected split-ring frequency selective surfaces. *IEEE Antennas and Wireless Propagation Letters*, 2014, vol. 13, p. 153 to 156. ISSN: 1536-1225. DOI: 10.1109/LAWP.2014.2298393

[11] HUANG, X., YANG, D., YANG, H. Multiple-band reflective polarization converter using U-shaped metamaterial. *Journal of Applied Physics*, 2014, vol. 115, no. 10, p. 103505. ISSN: 0021-8979. DOI: 10.1063/1.4868076

[12] MUTLU, M., AKOSMAN, A. E., SEREBRYANNIKOV, A. E., et al. Asymmetric chiral metamaterial circular polarizer based on four U-shaped split ring resonators. *Optics Letters*, 2011, vol. 36, no. 9, p. 1653–1655. ISSN: 0146-9592. DOI: 10.1364/OL.36.001653

[13] HAO, J., YUAN, Y., RAN, L., et al. Manipulating electromagnetic wave polarizations by anisotropic metamaterials. *Physical Review Letters*, 2007, vol. 99, no. 6, p. 063908. ISSN: 0031-9007. DOI: 10.1103/PhysRevLett.99.063908

[14] MA, X., HUANG, C., PU, M., et al. Multi-band circular polarizer using planar spiral metamaterial structure. *Optics Express*, 2012, vol. 20, no. 14, p. 16050–16058. ISSN: 1094-4087. DOI: 10.1364/OE.20.016050

[15] SHI, J., LIU, X., YU, S., et al. Dual-band asymmetric transmission of linear polarization in bilayered chiral metamaterial. *Applied Physics Letters*, 2013, vol. 102, no. 19, p. 191905. ISSN: 0003-6951. DOI: 10.1063/1.4805075

[16] XU, H., WANG, G., QI, M., et al. Compact dual-band circular polarizer using twisted Hilbert-shaped chiral metamaterial. *Optics Express*, 2013, vol. 21, no. 21, p. 24912–24921. ISSN: 1094-4087. DOI: 10.1364/OE.21.024912

[17] ZHU, W., RUKHLENKO, I. D., XIAO, F., et al. Polarization conversion in U-shaped chiral metamaterial with four-fold symmetry breaking. *Journal of Applied Physics*, 2014, vol. 115, no. 14, p. 143101. ISSN: 0021-8979. DOI: 10.1063/1.4870862

[18] SONG, K., ZHAO, X., LIU, Y., et al. A frequency-tunable 90°-polarization rotation device using composite chiral metamaterials. *Applied Physics Letters*, 2013, vol. 103, no. 10, p. 101908. ISSN: 0003-6951. DOI: 10.1063/1.4820810

[19] RAJKUMAR, R., YOGESH, N., SUBRAMANIAN, V. Cross polarization converter formed by rotated-arm-square chiral metamaterial. *Journal of Applied Physics*, 2013, vol. 114, no. 22, p. 224506. ISSN: 0021-8979. DOI: 10.1063/1.4846096

[20] FENG, M., WANG, J., MA, H., et al. Broadband polarization rotator based on multi-order plasmon resonances and high impedance surfaces. *Journal of Applied Physics*, 2013, vol. 114, no. 7, p. 074508. ISSN: 0021-8979. DOI: 10.1063/1.4819017

[21] SHI, H., LI, J., ZHANG, A., et al. Broadband cross polarization converter using plasmon hybridizations in a ring/disk cavity. *Optics Express*, 2014, vol. 22, no. 17, p. 20973–20981. ISSN: 1094-4087. DOI:10.1364/OE.22.020973

[22] ZHANG, L., ZHOU, P., LU, H., et al. Ultra-thin reflective metamaterial polarization rotator based on multiple plasmon resonances. *IEEE Antennas and Wireless Propagation Letters*, 2015, vol. 14, p. 1157–1160. ISSN: 1536-1225. DOI: 10.1109/LAWP.2015.2393376

[23] STUTZMAN, W. L., THIELE, G. A. *Antenna Theory and Design.* 2nd ed. Wiley Publishing, 1998. ISBN: 0471025909

About the Authors …

Zhao ZHANG was born in Baoji, Shaanxi province, P.R. China in 1990. He received B.S. and M.S. from Air Force Engineering University, Xi'an China, in 2012 and 2014. He is currently working toward Ph.D. degree at the Information and Navigation College of the Air Force Engineering University. His main interests include tilted beam antennas, circularly polarized antennas, metamaterial design and RCS reduction.

Xiangyu CAO received the B.Sc and M.A.Sc degrees from the Air Force Missile Institute in 1986 and 1989, respectively. She joined the Air Force Missile Institute in 1989 as an assistant teacher. She became an associate professor in 1996. She received Ph.D. degree from the Missile Institute of Air Force Engineering University in 1999. From 1999 to 2002, she was engaged in postdoctoral research in Xidian University, China. She was a Senior Research Associate in the Department of Electronic Engineering, City University of Hong Kong from Jun. 2002 to Dec. 2003. She is currently a professor of Air Force Engineering University of CPLA. Her research interests include computational electromagnetic, smart antennas, electromagnetic metamaterial and their antenna applications, and electromagnetic compatibility.